

STRUCTURAL STATE STUDY OF HIGH-PURITY TITANIUM AFTER SEVERE PLASTIC DEFORMATION AND CRYOGENIC QUASI-HYDROSTATIC EXTRUSION BY XRD METHODS

*E.E. Boklag, I.V. Kolodiy, M.A. Tikhonovsky, I.F. Kislyak, P.A. Khaimovich, A.A. Efimov
National Science Center "Kharkov Institute of Physics and Technology", Kharkov, Ukraine
E-mail: gao@ukr.net*

Nanocrystalline bulk high-purity titanium samples were obtained by combined severe plastic deformation SPD, thermal treatment and quasi-hydrostatic extrusion QHE at liquid nitrogen LNT and room RT temperatures. Texture and microstructural evolution of Ti have been investigated by XRD methods. The effect of initial structural state on deformation behavior of Ti after QHE was established. QHE of ultrafine-grained samples leads to structure formation, which parameters are independent on temperature of QHE. Significant differences in QHE process are observed for pre-annealed coarse-grained samples. These differences are related to deformation mechanisms, activated during the QHE process at LNT and RT.

1. INTRODUCTION

Titanium and titanium-based alloys are widely used materials for medical implants manufacturing due to its excellent biocompatibility, corrosion resistance and low ion-formation tendency in aqueous environment [1, 2]. Until recently, alloy materials were preferred (for example, Ti-6Al-4V), because of its higher mechanical properties in comparison with pure titanium. But the development level of the modern medicine has considerably higher material requirements. In spite of high biocompatibility and strength, titanium-based alloys usually contain toxic elements, which can provoke allergic reactions during implant healing process. For this reason researchers are taking an interest in pure titanium. Modern methods of severe plastic deformation (SPD) allow to obtain nanostructured and ultrafine-grained UFG titanium (commercially pure and high-purity), which has unique physical and mechanical properties. For this purpose different SPD methods were realized for commercially pure titanium, such as high pressure torsion (HPT) [3], equal channel angular extrusion (ECAE) [4–7], uniaxial compression [8], large-strain machining [9], cryogenic rolling [10]. Large degrees of true strain and heightened temperatures are usually required for production of UFG and nanocrystalline materials by afore-cited methods. But, at the same time, dynamical recovery effect appears. Besides, the combination of SPD methods results in better mechanical behavior of Ti samples [11]. Therefore, the main goal of this work was to study the structural state of high-purity titanium after SPD (compression-extrusion + wire drawing), thermal treatment and following quasi-hydrostatic extrusion at liquid nitrogen and room temperatures (QHE77K and QHE300K series, respectively).

2. MATERIALS AND METHODS

Iodide purity titanium after double electron-beam melting at a pressure ($P = 1.3 \cdot 10^{-4}$ Pa) was taken as an initial material. Combined severe plastic deformation was carried out in a few stages. At the first step preliminary compression-extrusion of the initial ingot was performed. The true strain aggregated a value of $e = 3.54$, after the deformation final billet was $\varnothing 10$ mm.

At the second stage, the extruded rod was drawn to diameter 5 mm at room temperature (total true strain after wire drawing was $e = 4.93$). The foregoing SPD methods are described in more detail in the article [12]. After this, the obtained bar was cut into the set of specimens. Some of them were annealed ($1.3 \cdot 10^{-1}$ Pa) at temperatures 150, 250, 300, 350, 450, 550 °C for 1 h to study an effect of the initial structural state on deformation behavior of Ti. Then samples after SPD and annealing were extruded by quasi-hydrostatic extrusion at liquid nitrogen LNT and room temperature RT. True strain after quasi-hydrostatic extrusion was $e \approx 0.86$. Quasi-hydrostatic extrusion method was developed in NSC KIPT and described by authors in the articles [13, 14], and its usage, applied to high-purity titanium deformation, – in the article [12].

Texture and structure parameters of samples were studied by XRD methods. Integral intensity, peak position, line profile shape and integral breadth were analyzed. X-ray diffraction patterns were collected in Cu-K α radiation with DRON-4-07 diffractometer, equipped with scintillation detector and nickel filter.

Texture analysis of the specimens was carried out by Rietveld refinement. Degree of preferred orientation determination (percentage of crystal grains, oriented with predetermined crystallographic plane $\{hkl\}$ normal to deformation direction) was performed by integral intensity analysis combined with March-Dollase approach [15]:

$$P_{hkl} = \sum_{i=1}^M (r^2 \cdot \cos \varphi_i + 1/r \cdot \sin^2 \phi_i)^{-3/2}, \quad (1)$$

where P_{hkl} – normalization factor for (hkl) peak intensity correction; M – multiplicity factor (hkl) plane; φ – angle between the reference direction and the normal of the individual lattice plane; r – refined parameter (part of grains, randomly oriented in the sample).

Microstructural effect study was performed by integral breadth analysis method. Separated values of coherent-scattering domains (CSD) size and microstrains were obtained using Williamson-Hall plot. The main operational formula of this method is:

$$\beta = \lambda/D \cdot \cos \theta + \eta \cdot \operatorname{tg} \theta, \quad (2)$$

β – physical peak broadening (experimentally observed broadening corrected for instrumental broadening); λ – radiation wavelength; D – crystallite size (volume weighted); η – residual mean square value of microstrains; θ – diffraction angle. Coarse-grained silicon powder (grain size $\sim 30 \mu\text{m}$) was used as an instrumental-standard specimen.

3. RESULTS

3.1. SPD BY COMPRESSION-EXTRUSION – WIRE DRAWING WITH FOLLOWING ANNEALING

After the SPD by compression-extrusion and wire-drawing at room temperature the sample's structure has practically equiaxed crystallites (CSD size is 70.4 nm along the bar axis and 92.8 nm in a cross-section, value of microstrains is 0.4%). Analysing intensity distribution of the diffraction lines in the sample, it can be concluded an [10.0] axial texture presence in non-annealed deformed sample (e.g. grains are oriented with [10.0] crystallographic directions along rod axis). This is typical crystallographic texture for titanium at uniaxial deformation.

During the annealing temperature increasing it is observed crystallite size exponential growth and microstrains reducing depending on temperature (Figs. 1, 2; Table 1). It should be noted, that microstrains decrease weakly on annealing, and just at $T = 450 \text{ }^\circ\text{C}$ stress relaxation occurs in specimens. More interesting results are observed for CSD size. The crystallite size increases weakly along the bar axis and just at $T = 550 \text{ }^\circ\text{C}$ it reaches values comparable to standard's one.

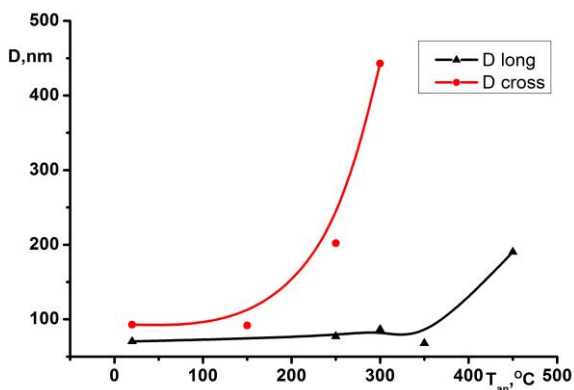


Fig. 1. CSD size dependence on annealing temperature in the samples after SPD

More intensive growth of crystallite size is observed in a cross-section of the bar depending on annealing temperature and at $T = 350 \text{ }^\circ\text{C}$ CSD size already reaches standard's level. Thus, crystallites have oblong shape, oriented normally to bar axis, up to $550 \text{ }^\circ\text{C}$. It should be noted, that annealing at $150 \text{ }^\circ\text{C}$ leads to slight CSD size decreasing in comparison with non-annealed deformed sample. This effect may be caused by anisotropy of coefficients of thermal expansion.

Peak (10.0) relative intensities are significantly higher in samples, annealed at temperatures from 150 to $350 \text{ }^\circ\text{C}$, then in non-annealed deformed sample. This indicates that the annealing samples are more textured

than non-annealed deformed sample. At higher annealing temperatures ($450, 550 \text{ }^\circ\text{C}$) texture randomization occurs and, at the same time, axial texture component [11.0] appears (typical annealing texture for titanium).

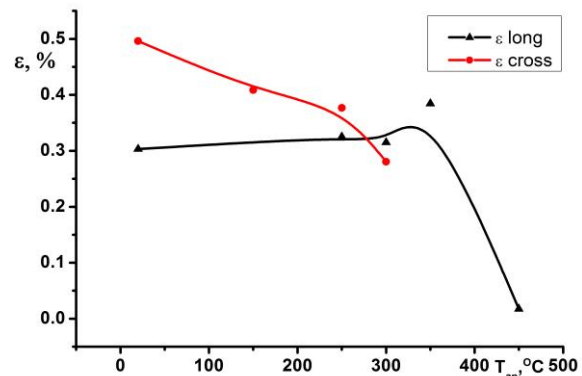


Fig. 2. Microstrains dependence on annealing temperature in the samples after SPD

Table 1
Dependence of Ti sub-structural parameters on annealing temperature after the SPD

$T_{\text{anneal}}, \text{ }^\circ\text{C}$	Cross-section		Longitudinal section	
	$D, \text{ nm}$	$\langle \epsilon \rangle$	$D, \text{ nm}$	$\langle \epsilon \rangle$
20	70.4	$3.03 \cdot 10^{-3}$	92.8	$4.96 \cdot 10^{-3}$
150	–	–	91.7	$4.59 \cdot 10^{-3}$
250	77.2	$3.25 \cdot 10^{-3}$	202.1	$3.77 \cdot 10^{-3}$
300	86.6	$3.15 \cdot 10^{-3}$	442.9	$2.81 \cdot 10^{-3}$
350	67.9	$3.84 \cdot 10^{-3}$	*	*
450	190.3	$1.7 \cdot 10^{-4}$	*	*
550	*	*	*	*

*Values of microstructural parameters are comparable to the instrumental-standard specimen's ones.

3.2. QUASI-HYDROSTATIC EXTRUSION AT ROOM AND NITROGEN TEMPERATURES

After the quasi-hydrostatic extrusion at LNT and RT practically the same values of sub-structural parameters are observed in deformed non-annealed samples (Table 2, $20 \text{ }^\circ\text{C}$). Thus CSD size is equal to $D \approx 62 \text{ nm}$, and the value of microstrains is a bit higher ($\langle \epsilon \rangle = 3.83 \cdot 10^{-3}$) in sample extruded at LNT as compared with extruded at RT one ($\langle \epsilon \rangle = 3.65 \cdot 10^{-3}$).

Pre-annealing temperature of SPD titanium has a significant effect on sub-structural parameters of quasi-hydrostatic extruded samples. For the pre-annealed samples after the QHE common tendency to microstrains decreasing is observed at annealing temperature decrease (Fig. 3, Table 2). Whereas the similar values of microstrains were obtained for both specimens' series (QHE77K and QHE300K). Concerning to CSD, exponential growth of crystallite size is observed in specimens, quasi-hydroextruded at room temperature (Fig. 4, 300 K series), with pre-annealing temperature increasing (crystallite size increased up to 136.2 nm at $T = 550 \text{ }^\circ\text{C}$).

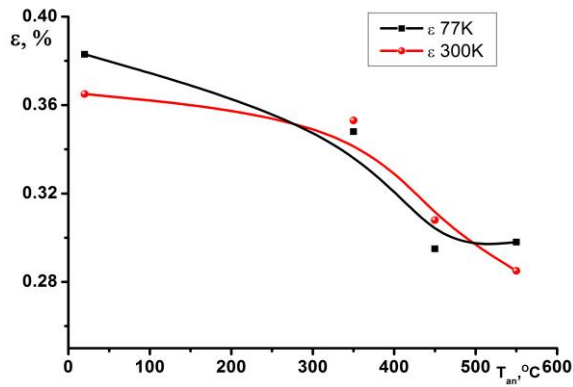


Fig. 3. Microstrains dependence on annealing temperature in the samples after QHE

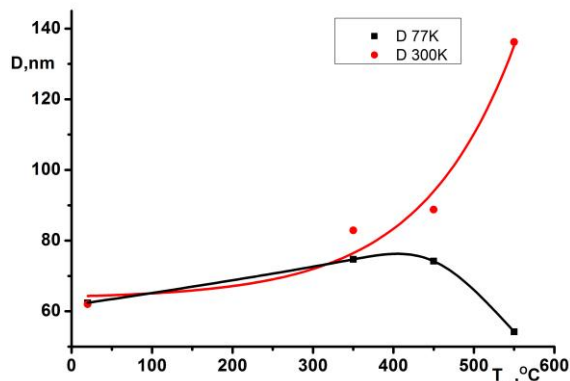


Fig. 4. CSD size dependence on annealing temperature in the samples after QHE

Table 2

Dependence of substructural parameters on pre-annealing temperature after the QHE

$T_{\text{anneal}},$ $^{\circ}\text{C}$	T_{QHE}			
	LNT		RT	
	D, nm	$\langle \epsilon \rangle$	D, nm	$\langle \epsilon \rangle$
20	62.4	$3.83 \cdot 10^{-3}$	62.0	$3.65 \cdot 10^{-3}$
350	74.7	$3.48 \cdot 10^{-3}$	82.9	$3.53 \cdot 10^{-3}$
450	74.2	$2.95 \cdot 10^{-3}$	88.8	$3.08 \cdot 10^{-3}$
550	54.2	$2.98 \cdot 10^{-3}$	136.2	$2.85 \cdot 10^{-3}$

Another situation is observed in the samples, deformed at nitrogen temperature (see Fig. 4, 77 K). In this case two pre-annealing temperature regions can be marked out, in which different tendencies of crystallite size changes are observed. Inside a temperature region up to 350 °C crystallite size grows up weakly with annealing temperature increasing (up to value $D = 74.7$ nm at $T = 350$ °C). In this region difference of CSD size is slight for samples, quasi hydroextruded at nitrogen and near-ambient temperatures, but it is visible that at $T = 350$ °C crystallites are bit smaller in QHE77K samples than in QHE300K ones. This difference becomes cardinal at higher pre-annealing temperatures; whereas the reverse trend is observed in samples extruded at nitrogen temperature – growth of pre-annealing temperature causes crystallite size decreasing (see Fig. 4, Table 2). So, minimal CSD size is obtained at $T = 550$ °C ($D = 54.2$ nm), which less than appropriate value even for non-annealed quasi-hydroextruded sample (62 nm).

In our opinion, so striking difference in crystallite size behavior can be related to the various mechanisms of titanium deformation at room and liquid nitrogen temperatures, as well as these mechanisms' dependence on grain size. It is known [16], that in HCP titanium $\langle a \rangle$ -type slip is a dominant mode of plastic deformation at room temperature (usually slip take place on $\{10.0\}$ first-order prism planes along the $\langle a \rangle$ direction). As temperature decreases the twinning mode considerably contributes to plastic deformation due to the limited number of slip systems in HCP metals and it can provide additional slip systems. It should be noted, that strength increases during the deformation twinning process due to the dislocation storage on the twins' boundaries [17]. Twinning propensity decreases for coarse-grained FCC and HCP metals with the grain size decreasing during deformation [18, 19]. At the same time temperature threshold, from which the twinning contributes essentially to deformation process, declines. So according to authors [20], during the deformation at LNT critical grain size, above which the twinning mechanism activates, is equal approximately 2 μm for titanium. (It should be kept in mind that increase of material purity promotes twinnability). As it shown earlier [21], investigated in this work titanium after SPD (compression-extrusion + wire-drawing) has ultrafine-grained or sub-microcrystalline structure (average grain size is about 150 nm). Annealing at temperatures till 300 °C practically doesn't influence the grain size. After the annealing at 350 °C bimodal structure with average grain sizes of 150 nm and 0.6 μm forms in specimens (individual grains can reach larger size). Annealing at 450 and 550 °C leads to the recrystallization process, thus microstructure with average grain size of 4 and 9 μm , respectively, is formed. Therefore, during the quasi-hydrostatic extrusion process of these samples at LNT twinning must be activated, especially in Ti, annealed at 550 °C. Direct conformation of this fact is the effect of QHE temperature on texture of the specimens, pre-annealed at different temperatures (Table 3). It is obvious, that the deformation temperature practically doesn't influence on the degree of the preferred orientations of sub-microcrystalline samples, obtained by SPD. Difference between r values for QHE77K and QHE300K samples increases with pre-annealing temperature growth. Less degree of texture of the samples after QHE77K is a consequence of twinning activation. During the twinning process grains fragmentation occurs and, therefore, different crystallographic orientations generates, providing specimens' texture randomization. This process of intensive grain fragmentation is responsible for the crystallite size decreasing in the samples, pre-annealed at 550 °C (see Fig. 4). From our point of view, observed crystallite size decreasing can explain non-monotonic microhardness and tensile strength dependencies of titanium after QHE77K on pre-annealing temperature, which can be observed in [12].

Based on the obtained results of the QHE temperature influence on CSD size and texture in SPD titanium, we can conclude the following. In HCP Ti twinning effect occurs during the SPD process of coarse-grained samples only and disappears in

nanocrystalline and UFG state. This conclusion adjusts with the authors' results [19], who also didn't observe twinning effect in nanocrystalline titanium, which is inherent to FCC metals [22, 23].

Table 3
Quasi-hydrostatic extrusion temperature (RT and LNT) influence on degree of texture (%) of the titanium samples, annealed at different temperatures

T _{QHE}	T _{anneal} , °C			
	20 °C	350 °C	450 °C	550 °C
LNT	72%	69%	58%	41%
RT	71%	74%	67%	57%

CONCLUSIONS

Texture and micro-structural investigations of high-purity Ti, obtained by combination of SPD (compression-extrusion + wire-drawing), thermal treatment and quasi-hydrostatic extrusion at nitrogen (QHE77K) and room temperatures (QHE300K) were made using X-ray diffraction methods.

It was established, that in the titanium after the SPD structure is formed, characterized by [10.0] axial texture presence. Crystallite size in this sample was $D = 70.4$ and 92.8 nm along the bar axis and in the cross-section, respectively. Value of microstrains was slightly higher in longitudinal section ($\langle \epsilon \rangle = 4.96 \cdot 10^{-3}$) than in cross-section ($\langle \epsilon \rangle = 3.03 \cdot 10^{-3}$).

In the preliminary deformed non-annealed samples, obtained by QHE at room and nitrogen temperatures, structural state is formed, parameters of which are practically independent on the QHE deformation temperature (degree of texture is $r \approx 0.7$ and CSD size is $D \approx 60$ nm, value of microstrains is $\langle \epsilon \rangle = 3.6 \dots 3.8 \cdot 10^{-3}$). At the same time, QHE deformation temperature has significant influence on the structural parameters of the samples after SPD and following recrystallization annealing at 450 and 550 °C. Quasi-hydrostatic extrusion at nitrogen temperature leads to more effective crystallite size grinding than the deformation at room temperature, especially in the coarse-grained samples. This is a consequence of the twinning activation at nitrogen temperature, which is an alternative deformation mechanism to dislocation slip. This assumption is confirmed by significant degree of texture decreasing in samples.

REFERENCES

1. C.N. Elias, J.H.C. Lima, R. Valiev, M.A. Meyers // *JOM*. 2008, v. 60, p. 46-49.
2. J. Klimas, M. Szota, M. Nabialek, A. Lukaszewicz, A. Bukowska // *J. Achieve. Mater. Manuf. Eng.* 2013, v. 61, p. 263.
3. R.Z. Valiev, A.V. Sergueeva, and A.K. Mukherjee // *Scripta Mater.* 2003, v. 49, p. 669.

4. I.P. Semenova, A.I. Korshunov, G.Kh. Salimgareeva, V.V. Latysh, E.B. Yakushina, and R.Z. Valiev // *The Physics of Metals and Metallography*. 2008, v. 106, p. 211.
5. G. Serra, L. Morais, C.N. Elias, I.P. Semenova, R. Valiev, G. Salimgareeva, M. Pithon, R. Lacerda // *Mater. Sci. Eng. C*. 2013, v. 33, p. 4197.
6. S.V. Sajadifar, G.G. Yapici // *Materials and Design*. 2014, v. 53, p. 749.
7. G. Purceka, O. Saraya, O. Kul, I. Karamanb, G. G. Yapici, M. Haouaoui, H.J. Maier // *Mater. Sci. Eng. A*. 2009, v. 517, p. 97.
8. E. Yu, I. Kim, D.H. Shin, and J. Kim // *Mat. Transact.* 2008, v. 49, p. 38.
9. M.R. Shankar, B.C. Rao, S. Lee, S. Chandrasekar, A.H. King, W.D. Compton // *Acta Mater.* 2006, v. 54, p. 3691.
10. I.S. Braude, N.N. Gal'tsov, V.A. Moskalenko, A.R. Smirnov // *Low Temp. Phys.* 2011, v. 37, p. 1042.
11. Z. Fan, H. Jiang, X. Sun, J. Song, X. Zhang, C. Xie // *Mater. Sci. Eng. A*. 2009, v. 527, p. 45.
12. M.A. Tikhonovsky, P.A. Khaimovich, K.V. Kutniy, I.F. Kislyak, V.S. Okovit, T.Yu. Rudycheva // *Low Temp. Phys.* 2013, v. 39, p. 1261.
13. P.A. Khaimovich // *Russian Physics Journal*. 2007, v. 50, p. 1079.
14. P.A. Khaimovich // *Perspective materials*. 2009, v. 3, p. 363.
15. W.A. Dollase // *J. Appl. Cryst.* 1986, v. 19, p. 267.
16. T.P. Chernyayeva, V.M. Grytsyna // *PAST. «Physics of Radiation Effect and Radiation Materials Science»*. 2008, N 2, p. 15.
17. A.A. Salem, S.R. Kalidindi, R.D. Doherty, S.L. Semiatin // *Met. Mater. Trans. A*. 2006, v. 37, p. 259.
18. E. El-Danaf, S.R. Kalidindi, and R.D. Doherty // *Met. Mater. Trans. A*. 1999, v. 30, p. 1223.
19. J.L. Sun, P.W. Trimby, F.K. Yan, X.Z. Liao, N.R. Tao, and J.T. Wang // *Scripta Mater.* 2013, v. 69, p. 428.
20. S.P. Malysheva, G.A. Salischev, R.M. Galeev, V.N. Danilenko, M.M. Myshlyayev, A.A. Popov // *The Physics of Metals and Metallography*. 2003, v. 95, p. 98.
21. M.A. Tikhonovsky, I.F. Kislyak, O.I. Volchok, T.Yu. Rudycheva, V.G. Yarovoy, A.V. Kuzmin, N.V. Kamyshanchenko, I.S. Nikulin // *High Pressure Physics and Technics*. 2008, v. 18, p. 96.
22. J.-Y. Zhang, G. Liu, R.H. Wang, J. Li, J. Sun, and E. Ma // *Phys. Rev. B*. 2010, v. 81, p. 172104.
23. S. Ni, Y.B. Wang, X.Z. Liao, H.Q. Li, R.B. Figueiredo, S.P. Ringer, T.G. Langdon, and Y.T. Zhu // *Phys. Rev. B*. 2011, v. 84, p. 235401.

Статья поступила в редакцию 14.08.2014 г.

ИССЛЕДОВАНИЕ СТРУКТУРНОГО СОСТОЯНИЯ ВЫСОКОЧИСТОГО ТИТАНА ПОСЛЕ ИНТЕНСИВНОЙ ПЛАСТИЧЕСКОЙ ДЕФОРМАЦИИ И КРИОГЕННОЙ КВАЗИГИДРОЭКСТРУЗИИ МЕТОДАМИ РЕНТГЕНОВСКОЙ ДИФРАКЦИИ

Е.Е. Боклаг, И.В. Колодий, М.А. Тихоновский, И.Ф. Кисляк, П.А. Хаймович, А.А. Ефимов

Методами комбинированной интенсивной пластической деформации, термообработок и квазигидроэкструзии (КГЭ) при азотной и комнатной температурах получены объемные нанокристаллические образцы высокочистого титана. Исследования текстуры и микроструктурных параметров титана проводились методами рентгеновской дифрактометрии. Установлено влияние исходного структурного состояния образцов на деформационное поведение титана при КГЭ. КГЭ ультрамелкозернистых образцов приводит к формированию структуры, параметры которой практически не зависят от температуры КГЭ. Значительные отличия наблюдаются в случае предварительно отожженных крупнозернистых образцов. Это связано с различными механизмами деформации (скольжением дислокаций и двойникованием), которые активируются в процессе КГЭ при комнатной и азотной температурах.

ДОСЛІДЖЕННЯ СТРУКТУРНОГО СТАНУ ВИСОКОЧИСТОГО ТИТАНУ ПІСЛЯ ІНТЕНСИВНОЇ ПЛАСТИЧНОЇ ДЕФОРМАЦІЇ І КРИОГЕННОЇ КВАЗІГІДРОЕКСТРУЗІЇ МЕТОДАМИ РЕНТГЕНІВСЬКОЇ ДИФРАКЦІЇ

О.Є. Боклаг, І.В. Колодій, М.А. Тихоновський, І.Ф. Кисляк, П.О. Хаймович, О.А. Єфімов

Методами комбінованої інтенсивної пластичної деформації, термообробок та квазигидроекструзії (КГЕ) при азотній та кімнатній температурах отримано нанокристалічні об'ємні зразки високочистого титану. Дослідження текстури та микроструктури титану проводилися методами рентгенівської дифракції. Встановлено вплив початкового структурного стану зразків на деформаційну поведінку титану при КГЕ. КГЕ ультрадрібнозернистих зразків призводить до формування структури з параметрами, незалежними від температури КГЕ. Значні відмінності спостерігаються у випадку попередньо відпалених крупнозернистих зразків. Це пов'язано з різними механізмами деформації (ковзанням дислокацій та двійнікуванням), що активуються під час КГЕ при кімнатній та азотній температурах.